Design of Low-Profile Integrated Transformer and Inductor for Substrate-Embedding in 1-5kW Isolated GaN DC-DC Converters

Haksun Lee, Vanessa Smet, P. M. Raj, Rao Tummala
3D Systems Packaging Research Center
Georgia Institute of Technology
Atlanta, USA
e-mail: hlee435@gatech.edu

***Abstract*— This paper presents the design analysis of low-profile transformers in 1-5kW DC-DC resonant converters. Recent advances in GaN devices are expected to improve the efficiency and power density of power converters, while the magnetics still remain the major bottleneck to miniaturization. A low-profile integrated magnetic component design that enables low-loss and high-power density is proposed for 400V/48V DC-DC resonant converters with 1kW output power. The winding loss, core loss, and power density of the novel magnetic component design is analyzed and compared with the conventional design approach using planar cores. Higher power density and lower loss are demonstrated with the novel design approach.**

Keywords-Low-profile; transformer; magnetics, embedding

I. INTRODUCTION

The recent rise of autonomous driving and electric vehicles has been driving a growing need for higher degree of electrification, and, consequently, for multiple levels of power conversion units. Isolated DC-DC converters are one of the essential building blocks in the power conversion chain which provide galvanic isolation between the input and output terminals. Isolated DC-DC converters face a challenge in increasing power density and efficiency due to their bulky size and lossy components. The most difficult design aspect of isolated DC-DC converters, such as resonant converters, has been magnetic components [1], since they account for a significant portion of the total converter losses and take up a large footprint on the converter substrate. Thus, transformer and inductor have been the critical hindrance to high-efficiency and miniaturization of isolated DC-DC converters. This paper focuses on low-profile design of magnetic components for isolated DC-DC converters with an increase in power density while not sacrificing the efficiency.

Two approaches are concurrently pursued for miniaturization of isolated DC-DC converters: one is increasing the switching frequency of the device, and the other is employing novel transformer technologies. In DC-DC power conversion, higher switching frequencies bring about a reduction in the volume of passive components such as inductors, transformers, and capacitors, which leads to higher power densities and lower cost of converters [2]. However, this increase in operating frequency is generally limited by the subsequent increase in power losses and permissible temperature of the power converter's components [3]. This has long been the technological bottleneck for miniaturization of Si-based power modules. Recent advances in GaN-on-Si power devices opened up various paths for innovation in isolated DC-DC converters. Numerous efforts are being made in research and industry to develop GaN-based converter prototypes which exploit the advantages of GaN in achieving higher power densities and efficiencies [1],[4],[5].

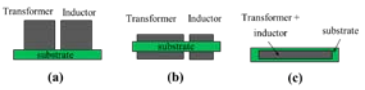

Figure 1. Magnetic components implementation schemes (a) Surface mounted configuration (b) Planar PCB integrated configuration (c) Low-profile embedded configuration.

Despite significant research progress in wide-bandgap devices, research innovations in magnetic component design are also necessary in order to futher increase the density and efficiency of power converters. Traditionally, transformer and inductor in isolated DC-DC converters have been mounted on substrate as discretes with individual cores for each wire-wound component as shown in Fig. 1 (a). These conventional wire-wound components are still widely used in industry products due to their well-established and straightforward design process, but they suffer from bulky size, low repeatability, and high profile. To increase power density and reduce the part count, various integrated magnetic designs were proposed [6] with monolithic integration of the inductor component into the transformer core by using either additional windings or the leakage inductance. However, these wire-wound designs are far from mass production processes which increases fabrication costs and degrades repeatablility. More recently, planar magnetic components, shown in Fig.1(b), have been widely investigated in 0.1 to 5kW range due to their advantages of low profile, high-power density, good thermal characteristic, and ease of manufacturability [7]. The planar designs are either implemented in discrete or integrated components. Examples of different components mentioned above are shown in Fig. 2.

Recent research activities in power package design

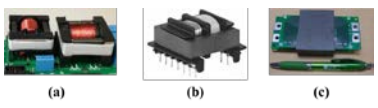

Figure 2. (a) Conventional discrete inductor and transformer [8] (b) integrated magnetics [9] (c) planar magnetics [10].

involve substrate embedding technologies. For low-power DC-DC converters ranging from 1 to 20 W, which have relatively simple toplogy and small number of components, magnetic components are integrated into a substrate to enable high-power density module packages [11]. Similarly, in the high-power side ranging from 5 ~ 50kW, gate driver circuits are integrated on top of the power plane by active power embedding for low-loss and high-density inverter module packages [12],[13]. However, for isolated DC-DC converters ranging from 0.1 to 5kW, which generally involve multiple magnetic components including transformers, there are no substrate embedding solutions to integrate the magnetic components due to their relatively bulky sizes. Therefore, a novel low-profile magnetics design, as shown in Fig. 1(c), needs to be developed in order to be compatible with the embedding trend of power modules.

This work addresses the aforementioned challenges with a novel design of transformer with integrated resonant inductor on a single magnetic core of less than 5mm in thickness with the following key innovations: (i) low-profile core and winding design reconciling loss and power density; (ii) insertion of magnetic slabs to widen the range of leakage inductance values and enable more standardized magnetics designs; (iii) ultra-thin package structure compatible with panel-scale power embedding processes. The following sections will describe the design analysis of ultra-low profile and substrate-integrated transformers and inductors applicable to high-frequency LLC resonant converters using GaN devices.

II. MODELING

A. *Isolated DC-DC Converter Using GaN*

LLC resonant converter is a popular topology for isolated DC-DC converters in high-voltage applications (400-600V) in the power range of 100 W - 5 kW [5]. The specifications of the converter that is used in this article are shown in Table 1. This section will briefly explain how the LLC resonant converter is structured, and summarize the necessary converter specifications for magnetics design.

Fig. 3 shows a simplified diagram of typical circuit topology for LLC resonant converters. The converter mainly consists of three building blocks: square wave generator, resonant network, and rectifier network. The square wave generator produces a square wave voltage from the DC source (Vin) by driving switches S1 and S2. In conventional converter designs, silicon power MOSFETs were used in this building block. However, in this paper, commercially available GaN FETs are employed in designing the converter for higher efficiency and miniaturization purposes [14].

TABLE I. CONVERTER SPECIFICATIONS

Parameter	Symbol	Value
Input voltage	Vin	350 - 400 V
Output voltage	Vout	48 V
Output power	Pout	1 kW

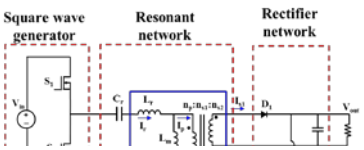

Figure 3. Schematic diagram of LLC resonant converter topology

The generated square wave voltage is applied to the resonant network which consists of resonant capacitor (Cr), resonant inductor (Lr), magnetizing inductor (Lm), and the transformer. Through this resonant network, the GaN FETs are turned on with zero voltage which allows low-loss switching of the power devices [9]. The magnetic components in the resonant network are either realized with discrete components (two separate cores as shown in Fig. 1(a)), or with integrated magnetics which combine resonant and magnetizing inductors on a single core. In this work, the components enclosed with a blue box in Fig. 3 are designed using a single integrated core.

The rectifier part rectifies the AC current coming from the resonant network and produces a DC output voltage with diodes and capacitor. This part can be implemented with full-wave bridge or center-tapped configuration. In this study, center-tapped configuration is selected in order to reduce the part count and device-related losses in the secondary-side.
Passive components should be carefully designed since they not only affect the overall size of the converter but also the switching and magnetic component-related losses. For instance, large Lm would reduce the current through the primary-side of the transformer and the inductor windings. As a result, the device loss, transformer core loss, and winding loss would decrease, but the magnetic component size would remain relatively large. Many different parameters need to be considered, and various procedures exist to optimize the LLC resonant converter design [3], [5], [9]. One design example with the converter specifications is summarized in Table. 2. This converter design is based on the LLC converter with GaN FET device, and follows the design procedure presented in reference [9].

TABLE II. SUMMARY OF CONVERTER DESIGN SPECIFICATIONS

Parameter	Symbol	Value
Resonant current (rms)	I_r	5.1 A
Magnetizing current (peak)	I_{Lmpk}	2.8 A
Secondary current (rms)	I_s	16.5 A
Switching frequency	f_s	325 kHz
Turns ratio of transformer	$n_p:n_{s1}:n_{s2}$	5:1:1
Resonant capacitor	C_r	31.0 nF
Resonant inductor	L_r	3.3 μH
Magnetizing inductor	L_m	65.4 μH

B. *Magnetic Component Design*

In LLC resonant converters, the magnetizing inductance of the transformer is usually implemented on a magnetic core with an air gap to meet the required inductance value. Fig. 4 shows the magnified schematic of magnetic components to be designed in this section. Since the secondary side of the transformer is a center-tapped structure, the turns ratio is selected to be 10:2:2.

The magnetic core structure with its geometrical parameters and the corresponding reluctance model used in this study are shown in Fig. 5. For better approximation of the inductance values of the reluctance model, the fringe fields of the air gap is taken into account according to the 3D calculation approach [15]. The flux generated by primary current Ip and secondary current Is cancel out, while the magnetizing current ILm produces common flux linking all windings. The expression for the maximum flux density in the core is shown in (1), where Ac is cross-sectional area of the core, and RTH is the total effective reluctance. Accurate prediction of the maximum flux density value is important to prevent saturation of the core. The final design

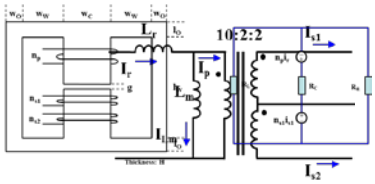

Figure 5. Magnetic core structure with geometrical parameters and its corresponding simplified reluctance model.

of the core should guarantee that the flux density value is lower than the maximum saturation value of the magnetic core material.

$$B_{max} = \frac{n_p \times I_{Lm\_pk}}{A_c \times R_{TH}} \quad (1)$$

Special care is needed when designing the windings since multiple windings are involved with mutual effect. Poor winding configurations would result in loose coupling between the windings, and end up with increased losses and leakage inductance. The thickness of the winding conductors should be selected considering the skin depth of the high-frequency current through the windings. Since AC current is restricted to the conductor surface, making the conducor thicker than the skin depth would not reduce the AC resistance [16]. The skin depth of copper at 325kHz is 110µm, and this thickness is used in windings of all of the magnetic components designed in this section.

As previously mentioned, the magnetic components can be implemented either with discrete components or integrated configuration. Design examples for both discrete and integrated cases will be presented in this section. Commercially available MnZn ferrite is selected as the core material based on the properties which showed lowest core loss and highest achievable power density in the frequency range of the interest [17].

The first design method is using discrete components to implement the resonant inductor and transformer as shown in Fig. 6. One planar core is used for the resonant inductor with windings, and another planar core is used for the transformer with primary winding and two secondary windings. Planar E core shapes were selected from the product catalog [18], and the reluctance model from the previous section is used in calculating the inductance values. Detailed core design rules are summarized in Table 3.

The windings of planar magnetics are generally fabricated using standard PCB processing which can easily be integrated with other circuit components through the wiring on the board. Fig. 7 presents the winding designs of the inductor and transformer. Interleaved configuration is applied in the transformer winding design in order to reduce

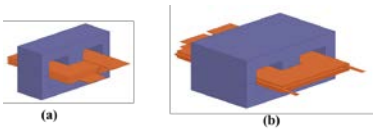

the leakage inductance. In this configuration, the primary

Figure 6. Discrete component designs using planar cores (a) resonant inductor (b) transformer.

TABLE III. DESIGN SUMMARY OF DISCRETE COMPONENTS

Parameter	Transformer	Resonant inductor
Core size	E 32/6/20	E 14/3.5/5
Material	MnZn	MnZn
Permeability μ_r	1400	1400
H	20.3 mm	5 mm
w_c	6.4 mm	3.0 mm
w_w	9.3 mm	4.0 mm
w_o	3.2 mm	1.5 mm
l_o	3.2 mm	1.5 mm
l_w	6.4 mm	4.0 mm
g	0.25 mm	0.1 mm

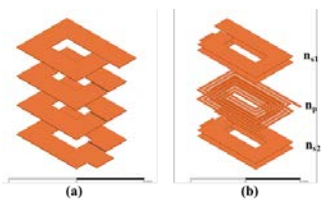

Figure 7. Winding configurations for discrete components (a) resonant inductor and (b) transformer.

winding is sandwitched in between the two secondary windings instead of arranging them all on one side.

The second design method is the novel proposed integrated design approach which combines the resonant inductor and the transformer into a single core, with an additional target of achieving a lowcore thickness for further miniaturatization of the converter. In this case, the leakage flux that exists between primary and secondary windings is utilized to implement the resonant inductor. However, the inherent leakage inductance of the transformer is generally not sufficient to meet the required resonant inductance value. Therefore, in this design, magnetic slabs are inserted in the window area between the primary and secondary winding to facilitate the control of the leakage inductance value. The slab material for leakage inductance can vary from low to high permeability materials as required.

In contrast to the previous design method using a standard core shape, the novel approach first selects the core thickness which is thin enough to be embedded into a power PCB substrate. Then, other parameters are decided through an iterative design process to meet the required magnetizing inductance value and resonant inductor value, while maintaining low loss and high density. A design summary for novel low-profile design in presented in Table 4, and its overall structure is shown in Fig. 8. As shown in Fig. 8(b) and (c), the primary winding is formed around the center leg of the magnetic core, while the secondary winding overlaps the primary winding with a controlled distance. The magnetic slab is introduced in the window area to separate primary and secondary windings. This separation, and insertion of magnetic slab, is to allow more leakage inductance to satisfy the resonant inductor value required for the circuit operation. The leakage inductance value can be adjusted by changing the separation distance of the two windings or replacing the magnetic slab with a different material.

TABLE IV. DESIGN SUMMARY FOR NOVEL LOW-PROFILE DESIGN

Parameter	Transformer
Core size	74 X 46 X 4 mm^3
Material	MnZn
Permeability μ_r	1400
H	4 mm
w_c	34 mm
w_w	3.0 mm
w_o	17 mm
l_o	17 mm
l_w	12 mm
g	0.24 mm

Parameter	Slab
Slab size	1.9 X 11 X 4 mm^3
Material	NiZn
Permeability μ_r	120

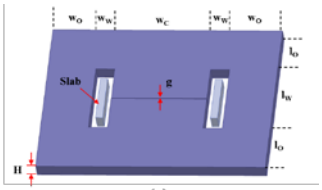

(a)

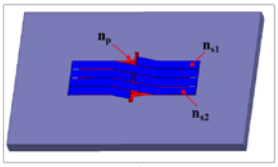
(b)

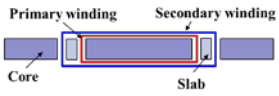

(c)

Figure 8. Overall structure of novel design; (a) core and slab dimensions, (b)

The two magnetics design approaches are then evaluated in terms of loss. The total magnetic component-related losses can be divided into copper winding losses and core losses. Core losses can be estimated using equation (2), where freq is the switching frequency, Bmax is maximum flux density, V is volume of the magnetic core, and Cm, CT, x, y are empirical parameters provided by core material manufacturers [19].

Winding losses can be expressed as equation (3) where I is the current through the winding, and Rac is the AC resistance of the winding conductor. Thus, the total winding losses in the discrete design are the sum of the losses from the resonant inductor winding, primary winding, and secondary winding of the transformer, whereas the total winding losses in the novel design only include losses from primary and secondary windings. The AC resistance values in practice are often measured with an impedance analyzer to calculate estimated winding losses. However in this paper, the AC resistance values are calculated using Q3D Extractor, a 3D parasitic extraction tool, with the winding designs obtained in this section.

Figure 9. Maxwell simulation results for inductance values

$$P_{core\_loss}=C_m \times C_T \times freq^x \times B_{max}^y \times 1e3 \times V \ [W] \quad (2)$$

$$P_{winding\_loss}=R_{ac}\times I^2 \ [W] \quad (3)$$

III. Results and Discussions

The simulation and loss calculation results of magnetic components designed in previous sections are presented in this section. The results of two different design methods will be compared in terms of loss and volume.

Fig. 9 shows ANSYS Maxwell simulation results for inductance values of magnetic components. All the values for discrete and integrated novel designs show good agreement with the required inductances. In other words, the designed parameters for magnetic core using the established reluctance model well predicted the required inductance values.

The calculated DC and AC resistances using Q3D extractor is summarized in Table 5. Although most of the resistances of the primary and secondary windings in both designs show similar ranges, the AC resistance of primary winding in the discrete design a has noticeable difference from that of the novel design. As shown in Fig. 7(b), the primary winding of discrete approach has to involve multiple windings in one layer with the winding trace width restricted by the window area. This restriction results in higher AC losses of the primary windings in the discrete approch.

Fig. 10 shows the calculated losses as well as the power densities of both discrete and integrated designs. The core losses in each design approach are calculated based on equation (2) with the loss estimation parameters provided by reference [19]. The novel low-profile design achieves ~40%

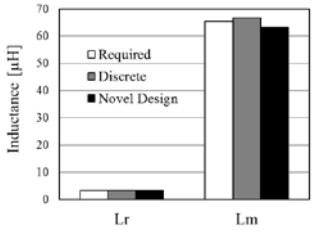

TABLE V. Simulation Results for Winding Resistances

Parameter		DC Resistance [mΩ]	AC Resistance [mΩ]
Discrete design	Winding of Lr	4.5	29.7
	Primary winding	117.0	564.0
	Secondary winding	3.0	19.7
Novel Design	Winding of Lr	N/A	N/A
	Primary winding	120.0	121.0
	Secondary winding	10.2	22.9

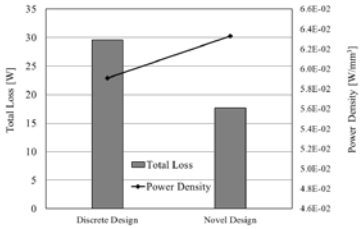

Figure 10. Calculated total losses and power densities with the two design approaches.

lower overall loss with a 7% increase in power density. The total core volume of discrete planar magnetics itself is smaller than the novel core design, but the overall volume of the two components, including the winding dimensions, exceeds the volume of the novel design. Another notable advantage of the novel design is the low core profile of less than 5mm. There could be numerous magnetic design options considering the trade-offs between efficiency and volume, but conventional solutions have limitations in reducing the core thickness. The suggested design approach succeeded in achieving a low-profile core without compromizing efficiency or power density.

IV. Conclusions

A novel low-profile design approch for magnetic components, applicable to 1-5kW isolated DC-DC converters with higher efficiency and miniaturization is demonstrated. Magnetic components for LLC resonant converters are designed to convert DC voltages from 400V to 48V with 1kW output power. Two different design approaches to implement one resonant inductor (3.3μH), and one transformer with magnetizing inductor (65.4μH) are evaluated.

The first uses conventional discrete design process with standard planar cores and PCB windings. The second approach is based on a novel low-profile core design which integrates the resonant inductor into the transformer by utilizing the leakage inductance. These discrete and novel approches are evaluated in terms of winding loss, core loss, and total volume of components. As a result, the novel design showed lower loss with improved power density.

The proposed magnetic design is in accordance with upcoming power embedding technologies, which can be a potential breakthrough in increasing power density and resolving aggravated thermal density challenges in future GaN-based power converters.

Acknowledgments

This work was supported by funding from the global industry consortium at the Georgia Tech 3D Systems Packaging Research Center. The authors are grateful to the industry sponsors and mentors for their funding and technical guidance.

References

$$P_{winding\_loss}=R_{ac}\times I^2 \ [W] \quad (3)$$

[1] M. D. Seeman, "GaN Devices in Resonant LLC Converters: System-level considerations," in *IEEE Power Electronics Magazine*, vol. 2, no. 1, pp. 36-41, March 2015.

[2] Z. Ouyang, O. C. Thomsen and M. A. E. Andersen, "Optimal Design and Tradeoff Analysis of Planar Transformer in High-Power DC–DC Converters," in *IEEE Transactions on Industrial Electronics*, vol. 59, no. 7, pp. 2800-2810, July 2012.

[3] Zhang, Jun. “Analysis and design of high frequency gapped transformers and planar transformers in LLC resonant converters.” Ph.D dissertation. 2015

[4] W. Zhang *et al*., "Evaluation and comparison of silicon and gallium nitride power transistors in LLC resonant converter," *2012 IEEE Energy Conversion Congress and Exposition (ECCE)*, Raleigh, NC, 2012, pp. 1362-1366.

[5] M. D. Seeman, S. R. Bahl, D. I. Anderson and G. A. Shah, "Advantages of GaN in a high-voltage resonant LLC converter," *2014 IEEE Applied Power Electronics Conference and Exposition - APEC 2014*, Fort Worth, TX, 2014, pp. 476-483.

[6] Y. Zhang, D. Xu, K. Mino and K. Sasagawa, "1MHz-1kW LLC Resonant Converter with Integrated Magnetics," *APEC 07 - Twenty-Second Annual IEEE Applied Power Electronics Conference and Exposition*, Anaheim, CA, USA, 2007, pp. 955-961.

[7] Ouyang, Ziwei. "Advances in planar and integrated magnetics." Ph.D dissertation. 2011.

[8] Wang, Haoyu. “Highly Efficient SiC Based Onboard Chargers for Plug-in Electric Vehicles.” Ph.D dissertation. 2014.

[9] Choi, Hangseok, and Power Conversion Team. "Design considerations for an LLC resonant converter." Fairchild Power Seminar. 2007.

[10] Rogers, Susan A. FY2013 Advanced Power Electronics and Electric Motors R&D Annual Progress Report. United States: N. p., 2014.

[11] Y. Su, W. Zhang, Q. Li, F. C. Lee and M. Mu, "High frequency integrated Point of Load (POL) module with PCB embedded inductor substrate," 2013 IEEE Energy Conversion Congress and Exposition, Denver, CO, 2013, pp. 1243-1250.

[12] Passmore, Brandon et al, “Three-dimensional packaging for wide bandgap based discrete and multi-chip power packages”, 25th Applied Power Electronics Conference and Exposition (APEC), 2014, Plenary session

[13] Neeb, Christoph, et al. "A 50 kW IGBT power module for automotive applications with extremely low DC-link inductance." 16th European Conference on Power Electronics and Applications (EPE'14-ECCE Europe), 2014.

[14] TPH3208 datasheet. (2016). [Online]. Available: http://www.transphormusa.com

[15] J. Muhlethaler, J.W Kolar, and A. Ecklebe, “A Novel Approach for 3D Air Gap Reluctance Calculations”, in Proc. Of the ICPE – ECCE Asia, Jeju, Korea 2011.

[16] Dixon, Lloyd. "Designing planar magnetics." Power Supply Design Seminar. 2006.

[17] Ferroxcube Data Handbook (2013). [Online]. Available: http://www.ferroxcube.com.

[18] Ferroxcube Product Selection Guide (2013). [Online]. Available: http://www.ferroxcube.com.

[19] New ER Cores for Planar Converters (2002). [Online]. Available: http://www.ferroxcube.com.